[3] P. Dunleavy and P. B. Katehi, "Shielding effects in microstrip discontinuities," *IEEE Trans. Microwave Theory Tech.*, vol. 36, pp. 1767–1774, Dec. 1988.

[4] T.-S. Horng, W. E. McKinzie, and N. G. Alexopoulos, "Full-wave spectral-domain analysis of compensation of microstrip discontinuities using triangular subdomain functions," *IEEE Trans. Microwave Theory Tech.*, vol. 40, pp. 2137–2148, Dec. 1992.

[5] J. C. Rautio and R. F. Harrington, "An electromagnetic time-harmonic analysis of shielded microstrip circuits," *IEEE Trans. Microwave Theory Tech.*, vol. MTT-35, pp. 726–730, Dec. 1987.

[6] H. Aubert, B. Souny, and H. Baudrand, "Origin and avoidance of spurious solutions in transverse resonance method," *IEEE Trans. Microwave Theory Tech.*, vol. 41, pp. 450–456, Mar. 1993.

[7] H. Baudrand, "Representation by equivalent circuit of the integral methods in microwave passive elements," in *20th European Microwave Conf. Proc.*, Budapest, Sept. 10–14, 1990, pp. 1359–1364.

[8] R. F. Harrington, *Time-Harmonic Electromagnetic Fields.* New York: McGraw-Hill, 1961, pp. 346–348.

[9] S. Pujol, H. Baudrand, and V. F. Hanna, "A new approach of the source method for characterization of planar structures," in *21st European Microwave Conf. Proc.*, Stuttgart, Sept. 9–12, 1991, pp. 1015–1020.

[10] M. Swaminathan, E. Arvas, T. K. Sarkar, and A. R. Djordjevic, "Computation of cutoff wavenumbers of TE and TM modes in waveguides of arbitrary cross sections using a surface integral formulation," *IEEE Trans. Microwave Theory Tech.*, vol. 38, pp. 154–159, Feb. 1990.

[11] T. Itoh, *Numerical Techniques for Microwave and Millimeter-Wave Passive Structures.* New York: Wiley, 1989.

[12] A. Hill and V. K. Tripathi, "An efficient algorithm for the three-dimensional analysis of passive microstrip components and discontinuities for microwave and millimeter-wave integrated circuits," *IEEE Trans. Microwave Theory Tech.*, vol. 39, pp. 83–91, Jan. 1991.

[13] Kirschning, *et al.*, "Measurement and computer aided modeling of microstrip discontinuities by an improved resonator method," in *MTT-S Int. Mic. Symp. Dig.*, 1983, pp. 495–497.

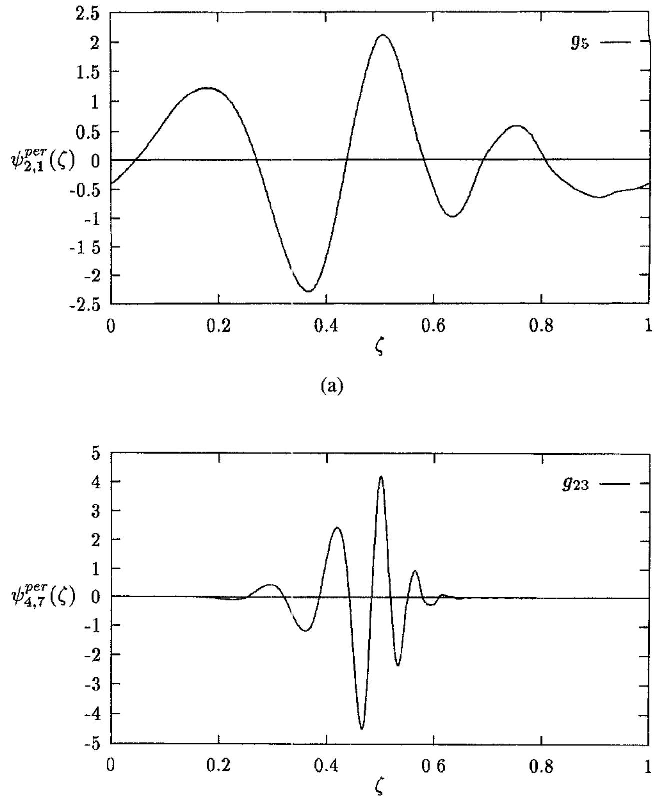


Fig. 1. The periodic wavelet constructed from the Daubechies orthogonal wavelet on the real line with $N = 7$. (a) $g_5(\zeta)\,[\psi^{per}_{2,1}(\zeta)]$ and (b) $g_{23}(\zeta)\,[\psi^{per}_{4,7}(\zeta)]$.

# On the Utilization of Periodic Wavelet Expansions in the Moment Methods

Gaofeng Wang

***Abstract*—In this short paper, a new wavelet approach that makes use of periodic wavelet expansions in the moment methods is presented. The unknown field or response is expanded in terms of the periodic wavelet functions. As a wavelet expansion method, the moment-method matrix is rendered sparsely populated after applying a threshold procedure. Moreover, this approach circumvents the difficulties in the application of the conventional wavelet expansions on the real line to finite interval problems. Numerical study shows that this approach gives better accuracy than the use of the conventional wavelet expansions on the whole real line.**

## I. Introduction

Recently, the wavelet expansion methods have been introduced to the applications of numerical analysis in electromagnetics (e.g., see [1]–[3]). Although the theory of wavelets is a relatively new area in mathematics, it has found many applications in engineering areas due to the special properties of wavelets. As a basis, the wavelet can be employed to express the unknown function in a series of wavelet functions. The wavelet expansion can adaptively fit itself to the various length scales associated with the physical configuration under study by distributing the localized basis functions near the discontinuities and the more spatially diffused ones over the smooth regions. Moreover, the cancellation property of the wavelets can eliminate, to a great extent, the coupling between the distant parts of the physical configuration under consideration. Attributed to these properties, the moment-method matrix obtained by a wavelet expansion is rendered sparsely populated as shown in [1]–[3].

Manuscript received August 26, 1994; revised June 29, 1995.
The author is with Tanner Research, Inc., Pasadena, CA 91107 USA.
IEEE Log Number 9414238.

However, difficulties exist when the unknown function is defined in finite intervals, while most of the wavelets are developed on the whole real line. In [1], Steinberg and Leviatan applied the Battle–Lemarie wavelet expansion on the real line to the moment method for solving an electromagnetic coupling problem [1]. Due to the infinite support of the Battle–Lemarie wavelet, the wavelet functions must be truncated to fit in the finite definition interval of the unknown function. The truncated wavelet basis lacks completeness over the finite interval under consideration. As a consequence, artificial oscillations appear in the results (e.g., see the magnitude of the equivalent magnetic current obtained from the truncated Battle–Lemarie wavelet in Fig. 4 of [1]).

A full wave analysis of microstrip floating line structures by wavelet expansion method was presented in [2], [3], where a Sommerfeld-type integral with an intractable kernel (the dyadic Green's functions for the grounded dielectric slab) was treated by using Daubechies wavelet. Since the Daubechies wavelet has compact support, one can easily delete the wavelet or scaling functions that are beyond the regions of interest, and thus the truncation of the

0018–9480/95$04.00 © 1995 IEEE

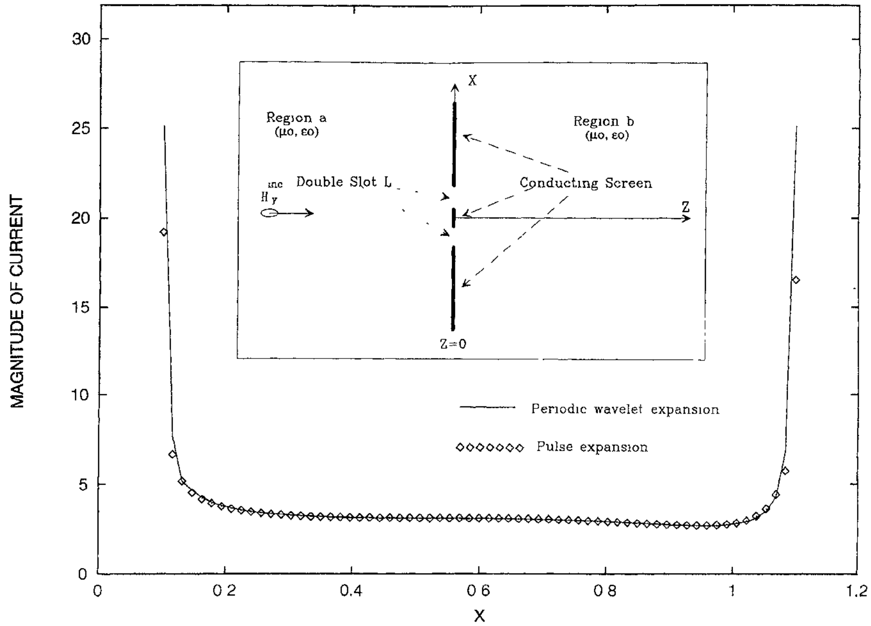


Fig. 2. Equivalent magnetic current magnitude obtained using the periodic wavelet expansion and the conventional pulse expansion.

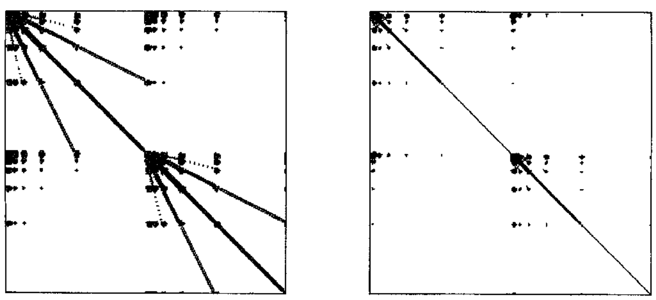

(a) (b)

Fig. 3. The sparseness structures of the moment-method matrix obtained by using the periodic wavelet expansion, (a) threshold $5 \times 10^{-4}$, $R \approx 7.74\%$ and (b) threshold $5 \times 10^{-3}$, $R \approx 2.08\%$.

wavelet at the boundary points is avoided. However, as mentioned in [2], [3], an edge basis is required at each end of the finite intervals to ensure the completeness of the basis.

Here, the periodic wavelets in $L^2([0, 1])$ are used in the moment methods instead of the wavelets on the whole real line. The utilization of periodic wavelets makes it possible to easily construct a complete basis over the finite interval. Numerical study shows that the artificial oscillations no longer occur.

## II. Theory

### A. Periodic, Orthogonal Wavelet

Given an orthogonal wavelet on the real line with scaling function (father wavelet) $\phi(\zeta)$ and mother wavelet $\psi(\zeta)$, a periodic, orthogonal wavelet can be constructed as [4]

$$\phi^{per}_{m,n}(\zeta) = \sum_{k \in \mathbf{Z}} \phi_{m,n}(\zeta + k) \quad (1)$$

$$\psi^{per}_{m,n}(\zeta) = \sum_{k \in \mathbf{Z}} \psi_{m,n}(\zeta + k) \quad (2)$$

where $\phi_{m,n}(\zeta) = 2^{m/2}\phi(2^m\zeta - n)$ and $\psi_{m,n}(\zeta) = 2^{m/2}\psi(2^m\zeta - n)$ are, respectively, the dilating and translating versions of the scaling function and mother wavelet, and $\mathbf{Z}$ is the set of integers. It can be shown that the following wavelet functions

$$g_0(\zeta) = \phi^{per}_{0,0}(\zeta) = 1 \quad (3)$$

$$\begin{aligned} g_{2^m+n}(\zeta) &= \psi^{per}_{m,n}(\zeta) \\ &= g_{2^m}(\zeta - n2^{-m}) \\ & 0 \le n \le 2^m - 1 \quad m = 0, 1, 2, \cdots \end{aligned} \quad (4)$$

constitute a periodic, orthonormal basis in $L^2([0, 1])$. For any periodic function $h(\zeta)$ in the interval [0, 1], an approximation of this function can be defined as the projection at resolution $2^m$

$$\begin{aligned} h(\zeta) &= P_m h(\zeta) \\ &= \sum_{n=0}^{2^m-1} h_n g_n(\zeta) \end{aligned} \quad (5)$$

where $h_n$ is the inner product of $h(\zeta)$ and $g_n(\zeta)$. The projection at resolution $2^m$ converges to the exact function as $m \to +\infty$.

From (1) and (2), the periodic wavelets can be constructed from their counterparts on the real line. The periodic, orthogonal wavelet constructed from the Daubechies compactly supported wavelet with $N = 7$ (see [4]) is plotted in Fig. 1.

### B. Periodic Wavelet Expansion in Moment Method

Consider the following linear integral equation

$$\int_L G(x, x')f(x')\,dx' = p(x), \quad x \in L \quad (6)$$

where $G(x, x')$ is the known kernel of the integral equation (usually the Green's function of the problem under consideration), $f(x')$ is the unknown function to be determined and $p(x)$ is the known excitation. Many electromagnetic scattering problems can be formulated in the above generic form. Usually, (6) is vectorial and two- or three-dimensional, but for the purpose here, it takes a scalar and one-dimension form. Generally, the integration domain $L$ consists of several line segments, namely, $L = \cup_{k=1}^{k=K} L_k$, where $K$ is the number of line segments, $L_k = [x_0^{(k)}, x_1^{(k)}]$ and $L_i \cap L_j = \emptyset$ if $i \neq j$.

If, further, it is assumed that $f(x')$ has the same behavior at the boundary points $x_0^{(k)}$ and $x_1^{(k)}$, i.e., $f[x_0^{(k)}] = f[x_1^{(k)}]$, the periodic

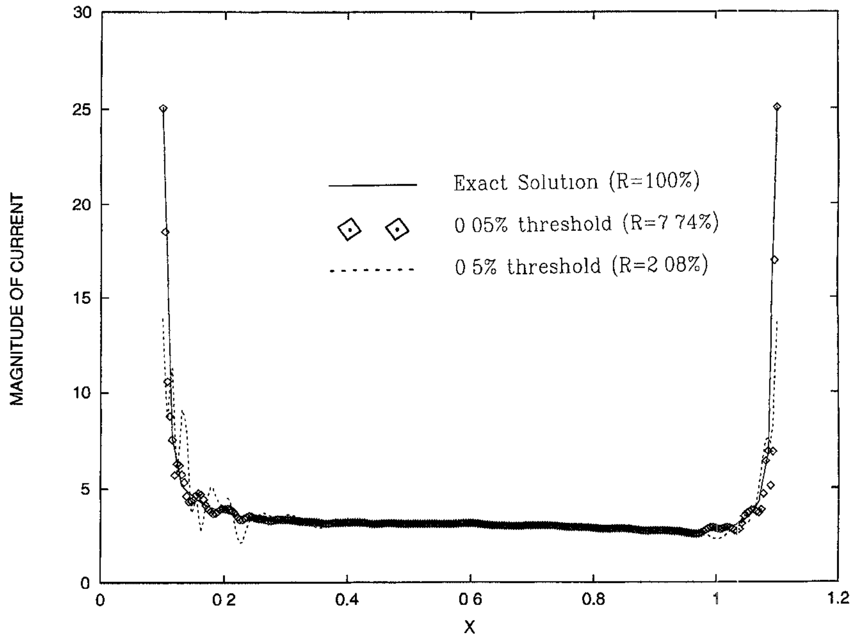


Fig. 4. Equivalent magnetic current magnitude obtained using the sparse matrices shown in Fig. 3.

wavelets can be adopted to express the unknown function over the line segment $L_k$ as long as one establishes a map between the line segment $L_k$ and the interval [0, 1]. Many practical electromagnetic problems are subjected to this constraint. In case this constraint is not satisfied, one can write the unknown function over segment $L_k$ in two terms: $f(x) = f^{(new)}(x) + Ce(x)$, where $e(x)$ is a *known* function which is defined over $L_k$ and satisfies the boundary conditions $e[x_0^{(k)}] = 0$ and $e[x_1^{(k)}] = 1$, and $C = f[x_1^{(k)}] - f[x_0^{(k)}]$. In fact, $e(x)$ can be selected in the same way as the basis functions in the conventional moment methods. For instance, $e(x)$ can be simply chosen as a pulse function near the boundary point $x_1^{(k)}$. If $f[x_0^{(k)}]$ and $f[x_1^{(k)}]$ are pre-defined, $C$ is a known constant. If $f[x_0^{(k)}]$ and $f[x_1^{(k)}]$ are unknown, $C$ can be considered as the expansion coefficient of the basis function $e(x)$. It is then determined in the same way as the other coefficients in the expansion of $f^{(new)}(x)$ by solving the moment-method matrix equation. By such a change of unknown function, it can easily be verified that the new unknown function $f^{(new)}(x)$ satisfies $f^{(new)}[x_0^{(k)}] = f^{(new)}[x_1^{(k)}]$. Therefore, without loss of generality, herein $f[x_0^{(k)}] = f[x_1^{(k)}]$ is assumed for each segment $L_k (k = 1, 2, \cdots, K)$.

Rewrite (6) as follows

$$\sum_{k=1}^{k=K} \int_{L_k} G(x, x') f(x')\, dx' = p(x), \qquad x \in L = \bigcup_{k=1}^{k=K} L_k. \tag{7}$$

A general procedure for solving the integral equation (7) is the moment method [5]. There are two sets of functions which completely specify a moment-method procedure. One is so-called basis functions and the other testing functions. Here, the periodic wavelet will be employed as both basis functions and testing functions. By using change of variables over segment $L_k$

$$x' = x_0^{(k)} + [x_1^{(k)} - x_0^{(k)}] \cdot \zeta' = T_k(\zeta') \tag{8}$$

(7) becomes

$$\sum_{k=1}^{k=K} \int_0^1 G[x, T_k(\zeta')]\, h^{(k)}(\zeta') |x_1^{(k)} - x_0^{(k)}|\, d\zeta' = p(x), \qquad x \in L = \bigcup_{k=1}^{k=K} L_k \tag{9}$$

where $h^{(k)}(\zeta) = f[T_k(\zeta)]$. Note that $h^{(k)}(\zeta)$ is defined on [0, 1] with $h^{(k)}(0) = h^{(k)}(1)$, thus it can be periodized to give a periodic function in $L^2([0, 1])$.

Using the periodic wavelet expansion (5) to $h^{(k)}(\zeta) (k = 1, 2, \cdots, K)$ and Galerkin's method for the testing procedure, a set of linear algebraic equations in matrix form can be obtained from integral (9) as follows

$$[A_{JN}] [H_N] = [B_J] \tag{10}$$

with

$$A_{JN} = \int_0^1 \left[ \int_0^1 G[T_k(\zeta), T_{k'}(\zeta')] g_n(\zeta') |x_1^{(k')} - x_0^{(k')}|\, d\zeta' \right] \cdot g_j(\zeta)\, |x_1^{(k)} - x_0^{(k)}|\, d\zeta$$

$$B_J = \int_0^1 p[T_k(\zeta)] g_j(\zeta)\, |x_1^{(k)} - x_0^{(k)}|\, d\zeta$$

$$H_N = h_n^{(k')}$$

where $j, n = 0, 1, 2, \cdots, 2^m - 1$, $J = (k-1) \cdot 2^m + j + 1$, and $N = (k' - 1) \cdot 2^m + n + 1$. The above integrations can be performed either using the conventional Gaussian quadrature or using the fast wavelet transform algorithm.

## III. Numerical Results

The problem of electromagnetic coupling through a double-slot aperture in a planar conducting screen separating two identical half-space regions is investigated in this section by using the *periodic* wavelet expansion. This problem was presented in [1] for the demonstration of the use of wavelet expansion on the real line in the moment method. To compare the two approaches, the same example with the same parameters is studied. Namely, $f(x) = M_y(x)$, $G(x, x') = H_0^{(2)}(2\pi\, |\, x - x'\, |\,)$, $p(x) = -[\eta_0/\pi]\, H_y^{inc}(x)$, $L = [-1.1, -0.1] \cup$

[0.1, 1.1], where $x$ is the physical coordinate normalized to wavelength, $M_y$ is the $y$-component of the equivalent magnetic current, $H_0^{(2)}$ is the zero-order, second-kind Hankel function, $\eta_0$ is the intrinsic impedance in free space, and $H_y^{inc}$ is the magnetic field intensity of the TE incident plane wave. Fig. 2 depicts the results of the magnitude of the equivalent magnetic current obtained using the periodic wavelet with $2^m = 128$ in comparison with the pulse function as the basis in moment method. The total number of periodic wavelet functions associated with the expansion with $2^m = 128$ is 256, as is also the total number of pulse functions used in the above computation. Good agreement can be observed between the two sets of results.

Unlike the case of the use of truncated wavelets on the real line in the moment method, where *strong* artificial oscillations almost definitely appear in the equivalent magnetic current magnitude near the boundary points no matter how high the resolution is selected in the wavelet expansion, the utilization of the periodic wavelets can suppress occurrences of oscillations near the boundary points as shown by Fig. 2. Due to the finite precision or resolution of computers and physical systems, solutions of problems under consideration are, in practice, represented in a finite resolution subspace. One major advantage of periodic wavelets is that, given a finite resolution $2^m$, there always exists a set of periodic wavelet functions that forms a complete basis in the corresponding subspace $\mathbf{V}_m^{per} \subset L^2([0, 1])$. By setting a map between the finite interval under study and [0, 1], one can obtain a complete basis defined on the desired computation domain from the periodic wavelets. Quite the contrary, it is very difficult for a set of truncated wavelet functions on the whole real line to form a complete basis in a finite interval. The occurrence of oscillations in the equivalent magnetic current magnitude is a consequence for the lack of completeness in the basis near the boundaries.

As was expected for a wavelet expansion method, the use of periodic wavelets renders a sparse moment-method matrix. To examine the sparsity, a threshold procedure is imposed on the moment-method matrix. That is, in the moment-method matrix, the element is kept only if its magnitude relative to that of the largest one is above a selected threshold and set to zero otherwise. Fig. 3 illustrates the sparseness structures of the moment-method matrix obtained by using this technique with thresholds of $5 \times 10^{-4}$ and $5 \times 10^{-3}$, where the black ink indicates the remaining nonzero elements. The ratio $R$ of the number of the remaining nonzero elements to the total number of elements can be obtained as $R \approx 7.74\%$ and $R \approx 2.08\%$ for the respective thresholds selected above. Fig. 4 shows the magnitude of the equivalent magnetic current obtained by using the sparse matrices in Fig. 3. Note that with the threshold $5 \times 10^{-4}$, the number of the matrix elements drastically reduces to $R \approx 7.74\%$ after the threshold processing. Although only such a small ratio of matrix elements is employed, the resultant equivalent magnetic current is still quite accurate as shown by Fig. 4. When the threshold $5 \times 10^{-3}$ is applied and the number of the used matrix elements further reduces to $R \approx 2.08\%$, some modest losses of accuracy appear near the boundaries in the resultant equivalent magnetic current as shown in Fig. 4. Considering that only a very small ratio (2.08%) of the matrix elements is used in this computation, the result is reasonably accurate.

## IV. Conclusion

The utilization of periodic wavelet expansions in the moment methods has been proposed here. Comparing with their counterparts on the real line, the periodic wavelets are more suitable to handle the finite interval problems since they bypass the difficulties arising in the use of wavelets on the whole real line to expand the unknown functions defined over finite intervals. The periodic wavelet expansion preserves the capability of generating sparse moment-method matrix and adaptively fits itself to the various length scales. Numerical example shows that the periodic wavelet expansion gives better accuracy than the conventional wavelet expansion for finite interval problems.

## References

[1] B. Z. Steinberg and Y. Leviatan, "On the use of wavelet expansions in the method of moments," *IEEE Trans. Antennas Propagat.*, vol. 41, pp. 610–619, May 1993.
[2] G. Wang and G. Pan, "Full wave analysis of microstrip floating line structures by wavelet expansion method," *IEEE Trans. Microwave Theory Tech.*, vol. 43, pp. 131–142, Jan. 1995.
[3] G. Wang, "Numerical techniques for electromagnetic modeling of high speed circuits," Ph.D. dissertation, Univ. of Wisconsin, Milwaukee, Oct. 1993.
[4] I. Daubechies, *Ten Lectures on Wavelet.* Philadelphia: SIAM Press, 1992.
[5] R. F. Harrington, *Field Computation by Moment Methods.* New York: IEEE Press, 1993.

# Analytical Expressions for Simplifying the Design of Broadband Low Noise Microwave Transistor Amplifiers

Garry N. Link and V. S. Rao Gudimetla

***Abstract*—An analytical expression for the minimum achievable noise figure for a specified gain at a given frequency is derived for a microwave amplifier. The minimum noise figure is given in terms of the specified gain, the amplifier noise parameters, and the S parameters. Similarly, another expression for the maximum gain at a specified noise figure is derived in terms of the noise figure, the noise parameters, and the S parameters. It is shown that these expressions simplify the tradeoff considerations for broadband low noise amplifier design by avoiding the need to draw several constant noise and gain circles at each frequency of interest.**

## I. Introduction

A broadband low noise amplifier is designed to meet a specified gain versus frequency profile, usually either flat gain or 6 dB/octave gain increase. The maximum acceptable noise figure over the entire bandwidth is also specified. To determine the minimum noise figure for the specified gain at a given frequency, the required gain circle is drawn on the Smith chart along with several noise figure circles [1], [2]. The minimum noise figure corresponds to the noise circle that is tangential to the gain circle. This process is repeated at each frequency of interest to ensure that the specified gain can be provided at or below the desired noise figure over the desired bandwidth. If not, a different device must be chosen or an additional tradeoff must

Manuscript received October 11, 1994; revised June 29, 1995.
G. N. Link was with Tektronix, Inc., MS 39-615, Beaverton, OR 97077-0001 USA. He is now with Maxim Integrated Products, Inc., Beaverton, OR 97005–1155 USA.
V. S. R. Gudimetla is with the Oregon Graduate Institute of Science and Technology, Department of EE/AP, Portland, OR 97291-1000 USA.
IEEE Log Number 9414239.